JANUSZ CEBULSKI
ORCID: 0000-0002-3813-8705

Silesian University of Technology, Faculty of Materials Engineering, Katowice, Poland

DOI: 10.15199/40.2023.6.2

High-temperature oxidation of $Fe_{40}Al_5Cr_{0.2}ZrB$ and TiAl intermetallic phase alloys

Wysokotemperaturowe utlenianie stopów na osnowie fazy międzymetalicznej $Fe_{40}Al_5Cr_{0,2}ZrB$ i TiAl

A comparison of high-temperature corrosion resistance was carried out between $Fe_{40}Al_5Cr_{0.2}ZrB$ intermetallic phase-based alloy and TiAl alloy by annealing in air at 1000°C for 50 h, 100 h, 200 h, and 500 h. The extent of oxide scale formation on the surface of both alloys was determined and related to the initial surface condition before the oxidation process. The surfaces of both materials were analyzed and compared after the same annealing time. The surface condition before and after oxidation was examined using a stereoscopic microscope. The kinetics of the oxidation process at 1000°C over a period of 500 h were determined. Samples after oxidation were observed using a Hitachi S-4200 scanning electron microscope. Additionally, energy-dispersive X-ray spectroscopy (EDS) was performed to analyze the chemical composition of all tested samples of both materials after oxidation. The relationship between the occurrence of corrosion products for each of the tested materials and the annealing time was demonstrated.

Keywords: FeAl, TiAl, corrosion, high-temperature corrosion, scale, Al_2O_3 oxide

W pracy dokonano porównania odporności na korozję wysokotemperaturową stopu na osnowie fazy międzymetalicznej $Fe_{40}Al_5Cr_{0,2}ZrB$ i stopu TiAl poprzez wyżarzanie w powietrzu w temperaturze 1000°C przez 50 h, 100 h, 200 h i 500 h. Określono powierzchnię zgorzeliny tlenkowej obu stopów i odniesiono te dane do stanu powierzchni przed procesem utleniania. Przeanalizowano i porównano powierzchnie obu materiałów po jednakowym czasie wyżarzania. Badania stanu powierzchni przed utlenianiem i po utlenianiu wykonano za pomocą mikroskopu stereoskopowego. Wyznaczono kinetykę procesu utleniania w temperaturze 1000°C w czasie 500 h. Próbki po procesie utleniania obserwowano przy użyciu elektronowego mikroskopu skaningowego Hitachi S-4200. Przeprowadzono również mikroanalizę rentgenowską składu chemicznego (EDS) wszystkich badanych próbek obu materiałów po utlenianiu. Wykazano zależność między występowaniem produktów korozji każdego z badanych materiałów a czasem wyżarzania.

Słowa kluczowe: FeAl, TiAl, korozja, korozja wysokotemperaturowa, zgorzelina, tlenek Al_2O_3

1. Introduction

Hot corrosion, resulting from the action of combustion products such as sulfur and chlorine compounds originating from vehicle exhaust gases and the combustion of fossil fuels in power plant boilers [1, 2], is a hazardous phenomenon. Consequently, alloys belonging to the innovative and advanced structural materials group, which are based on ordered intermetallic phases, have been investigated in recent years [3].

The most commonly studied and commercially utilized alloys based on intermetallic phases are those from the Fe-Al and Ti-Al systems. For economic reasons, the most popular alloys are iron-aluminum-based alloys, such as Fe_3Al and FeAl.

The selection of alloys for the study was guided by the fact that $Fe_{40}Al_5Cr_{0.2}ZrB$ alloy has been the subject of numerous studies, including corrosion resistance tests, during which selective oxidation of aluminum was observed. Meanwhile, studying the oxidation of the binary TiAl alloy would provide comparative information regarding the oxide morphology in a material belonging to the same group of engineering materials. From among the group of alloys based on titanium aluminides, the TiAl alloy with a stoichiometric composition based on the intermetallic phase was used as a reference material to obtain preliminary comparative information on the oxidation of this alloy and the $Fe_{40}Al_5Cr_{0.2}ZrB$ alloy under the same conditions. The properties of intermetallic phases cannot be predicted by summing up the properties of the two elements comprising the phase. Therefore, obtaining a more comprehensive characterization of these phases requires research focused on determining their properties, including high-temperature oxidation resistance [3–6].

2. Experimental

The material for the study consisted of samples 22 mm × 10 mm in size made from $Fe_{40}Al_5Cr_{0.2}ZrB$ alloy and from stoichiometric TiAl alloy (Table 1). After grinding with 800-grit paper, the samples were cleaned with isopropyl alcohol using an ultrasonic cleaner. Material melting was carried out in a Balzers vacuum induction furnace (VSG). Pure components, namely technically pure armco iron and 99.99% pure aro aluminum, as well as 99.5% pure titanium, were used for melting. The following research tasks were performed:

Janusz Cebulski, BEng, PhD, is a graduate of the Faculty of Materials Engineering, Metallurgy, Transport and Management of the Silesian University of Technology. He works as an assistant professor at the Faculty of Materials Science and Metallurgy at the Silesian University of Technology. His areas of research interest include alloys based on intermetallic compounds, in particular from the Fe–Al system, material structure studies, scanning electron microscopy, and cracking of materials.

E-mail: janusz.cebulski@polsl.pl

Otrzymano / Received: 15.03.2023. Przyjęto / Accepted: 17.05.2023

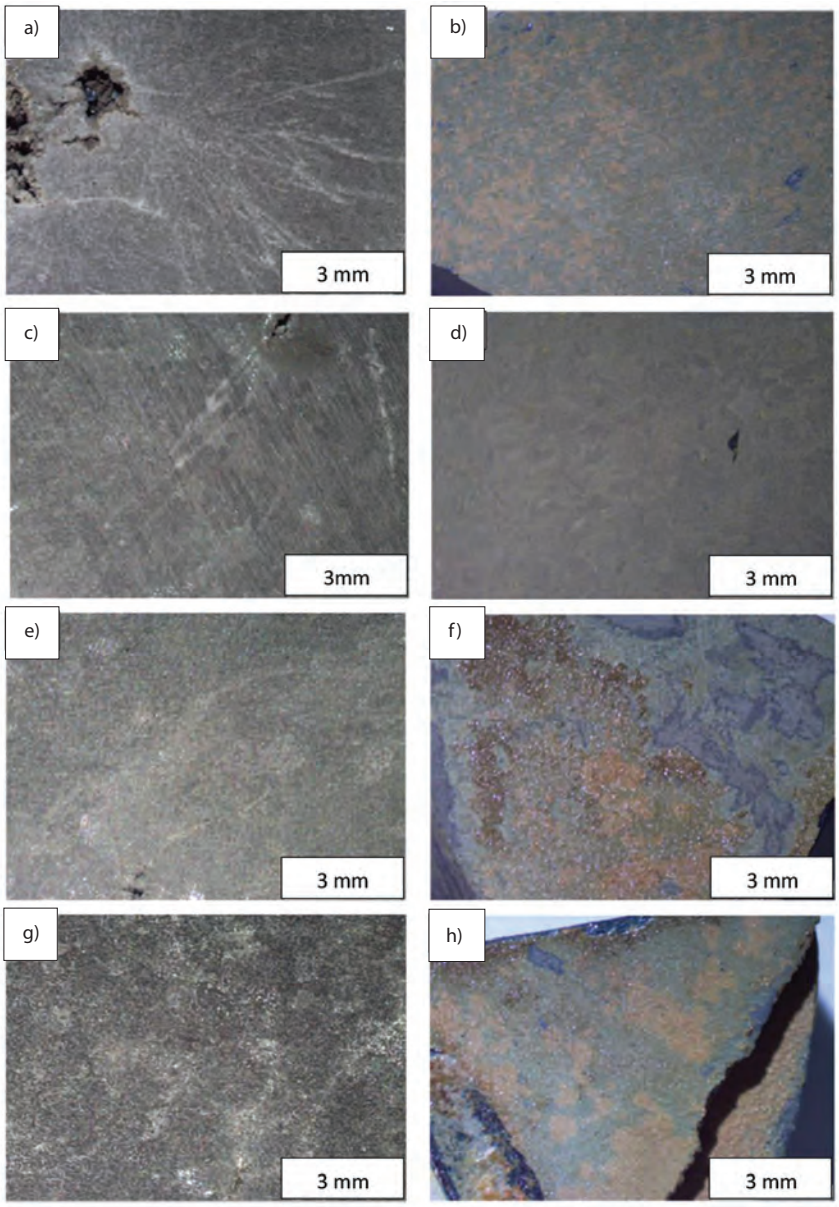

Fig. 1. Alloy surface after oxidation at 1000°C observed under a stereoscopic microscope: a) $Fe_{40}Al_5Cr_{0.2}ZrB$ after 50 h, b) TiAl after 50 h, c) $Fe_{40}Al_5Cr_{0.2}ZrB$ after 100 h, d) TiAl after 100 h, e) $Fe_{40}Al_5Cr_{0.2}ZrB$ after 200 h, f) TiAl after 200 h, g) $Fe_{40}Al_5Cr_{0.2}ZrB$ after 500 h, h) TiAl after 500 h

Rys. 1. Powierzchnia stopu po utlenianiu w temperaturze 1000°C zaobserwowana pod mikroskopem stereoskopowym: a) $Fe_{40}Al_5Cr_{0.2}ZrB$ po 50 h, b) TiAl po 50 h, c) $Fe_{40}Al_5Cr_{0.2}ZrB$ po 100 h, d) TiAl po 100 h, e) $Fe_{40}Al_5Cr_{0.2}ZrB$ po 200 h, f) TiAl po 200 h, g) $Fe_{40}Al_5Cr_{0.2}ZrB$ po 500 h, h) TiAl po 500 h

– Oxidation at a temperature of 1000°C for 50 h, 100 h, 200 h, and 500 h in air in a resistively heated chamber furnace made from Carbolite.
– Determination of oxidation kinetics using a discontinuous method.
– Surface observations using a stereoscopic microscope.
– Surface observations of the oxide layer on the samples using a Hitachi S-4200 scanning electron microscope (SEM) equipped with secondary electron detectors (SE). The observations were conducted at an accelerating voltage of 20 kV.
– Chemical composition analysis of the oxidation products using an energy-dispersive X-ray spectrometer (EDS) by Thermo Noran (System Six) at an electron beam accelerating voltage of 20 keV, coupled with the Hitachi S-4200 microscope.

Table 1. Chemical composition of the studied $Fe_{40}Al_5Cr_{0.2}ZrB$ and TiAl alloys
Tabela 1. Skład chemiczny badanych stopów $Fe_{40}Al_5Cr_{0,2}ZrB$ i TiAl

Alloy	Chemical composition [wt%]					
	Ti	Fe	Al	Cr	Zr	B
$Fe_{40}Al_5Cr_{0.2}ZrB$	–	the rest	23.69	5.69	0.19	0.015
TiAl	71.53	–	28.47	–	–	–

3. Experimental study results

3.1. Alloy surface morphology after oxidation as observed by stereoscopic microscopy and oxidation kinetics

Observations conducted using a stereoscopic microscope allowed for preliminary determination of the morphology of oxidation products formed on the surface of the examined alloys. The results of the observations are presented in Fig. 1. The surface condition of the samples after oxidation for up to 100 h remained practically unchanged (Fig. 1a–1d). It was found that after oxidation, the FeAl intermetallic phase-based alloy sample exhibited a more homogeneous layer of oxidation products (Fig. 1e, 1g) compared to the TiAl alloy sample, especially after oxidation for 200 h and 500 h (Fig. 1f, 1h). Cracks were also observed on the surface of TiAl alloy, while no cracks were observed on the surface of FeAl intermetallic phase-based alloy during observations using the stereoscopic microscope for any of the stated oxidation times. Determining the morphology of corrosion products using a stereoscopic microscope is not possible, therefore, based on the described experiments, specific locations were selected for observation using an electron scanning microscope. The oxidation kinetics of the tested materials were determined discontinuously

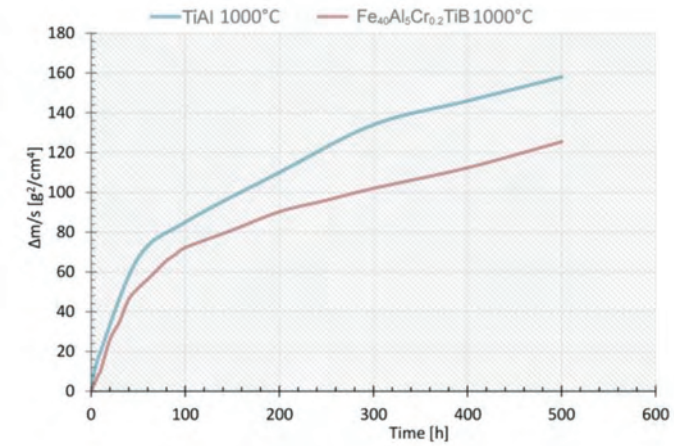

Fig. 2. Corrosion kinetics of $Fe_{40}Al_5Cr_{0.2}ZrB$ alloy and TiAl alloy after oxidation at 1000°C for up to 500 h

Rys. 2. Kinetyka korozji stopu $Fe_{40}Al_5Cr_{0,2}ZrB$ oraz stopu TiAl po utlenianiu w temperaturze 1000°C w czasie do 500 h

by measuring the mass of samples placed in a crucible to avoid mass changes caused by detachment of oxidation products, which is particularly important in the case of $Fe_{40}Al_5Cr_{0.2}ZrB$ alloy as the oxide layer tends to spall off during cooling due to thermal stress. It has been demonstrated that $Fe_{40}Al_5Cr_{0.2}ZrB$ alloy exhibits higher oxidation resistance at a temperature of 1000°C for up to 500 h [7]. Comparison of the corrosion kinetics of the tested alloys is presented in Fig. 2.

3.2. Alloy surface morphology after oxidation observed by scanning electron microscopy together with EDS microanalysis of chemical composition

Observations under the scanning electron microscope were carried out to determine differences in the morphology of corrosion products of the tested materials depending on the oxidation process time. In the case of both FeAl and TiAl intermetallic phase alloys, the surface of the tested material was covered with a layer of scale with heterogeneous morphology. Areas where the scale had chipped or flaked were visible (Fig. 3c, 3e, 3g). The oxide was characterized by an needle-like morphology, and lumpy crystallites were also noticeable. Examination of the $Fe_{40}Al_5Cr_{0.2}ZrB$ alloy subjected to oxidation for 100 h revealed that the oxide layer had begun to shed. Fragments of chipped scale and microcracks of the oxidized layer were observed. Fig. 3d shows the oxide morphology: sparse lumps, with needle-like and lamellar structures still predominating.

In the microstructural images of the sample oxidized for 200 h, it can be observed that in places where the top oxide layer is missing, successive oxide layers are present.

The largest area of oxidation product loss was observed for a sample exposed to an oxidizing environment for 500 h. The oxide scale filled the surface of the sample, although there was local chipping of the oxide layer.

The oxidation surface of the TiAl alloy was more homogeneous in terms of the structure of the oxide layer, but unlike the surface of FeAl intermetallic phase-based alloy, it did not have a lamellar structure which could flake off from the parent material.

X-ray microanalysis of the chemical composition showed that despite differences in the morphology of the oxidation products of both FeAl and TiAl phase alloys, aluminum was selectively oxidized, forming a passive Al_20_3 layer on the surface (Fig. 4). Due to the test methodology used, the oxygen concentration should be considered an estimate, and in the case studied, mostly aluminum and oxygen were found. Consequently, oxygen was not omitted during

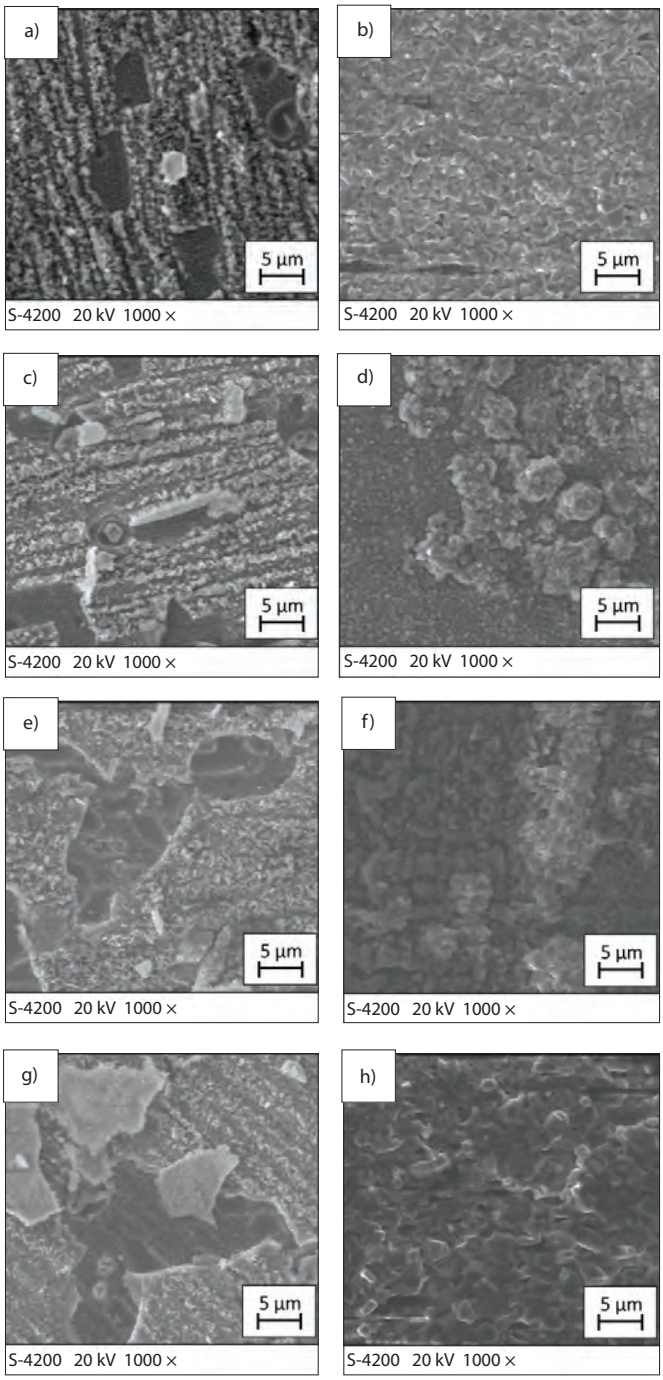

Fig. 3. Alloy surface after oxidation at 1000°C observed under a scanning electron microscope: a) $Fe_{40}Al_5Cr_{0.2}ZrB$ after 50 h, b) TiAl after 50 h, c) $Fe_{40}Al_5Cr_{0.2}ZrB$ after 100 h, d) TiAl after 100 h, e) $Fe_{40}Al_5Cr_{0.2}ZrB$ after 200 h, f) TiAl after 200 h, g) $Fe_{40}Al_5Cr_{0.2}ZrB$ after 500 h, h) TiAl after 500 h

Rys. 3. Powierzchnia stopu po utlenianiu w temperaturze 1000°C zaobserwowana pod elektronowym mikroskopem skaningowym: a) $Fe_{40}Al_5Cr_{0,2}ZrB$ po 50 h, b) TiAl po 50 h, c) $Fe_{40}Al_5Cr_{0,2}ZrB$ po 100 h, d) TiAl po 100 h, e) $Fe_{40}Al_5Cr_{0,2}ZrB$ po 200 h, f) TiAl po 200 h, g) $Fe_{40}Al_5Cr_{0,2}ZrB$ po 500 h, h) TiAl po 500 h

the quantitative analysis. From a stoichiometric point of view, and as seen in previous studies [8], the only oxide that can be formed is Al_2O_3 (iron comes from the substrate – due to the volumetric nature of the EDS measurement).

4. Summary

Analysis of the experimental results shows that the TiAl alloy sample surface had the most homogeneous scale structure after

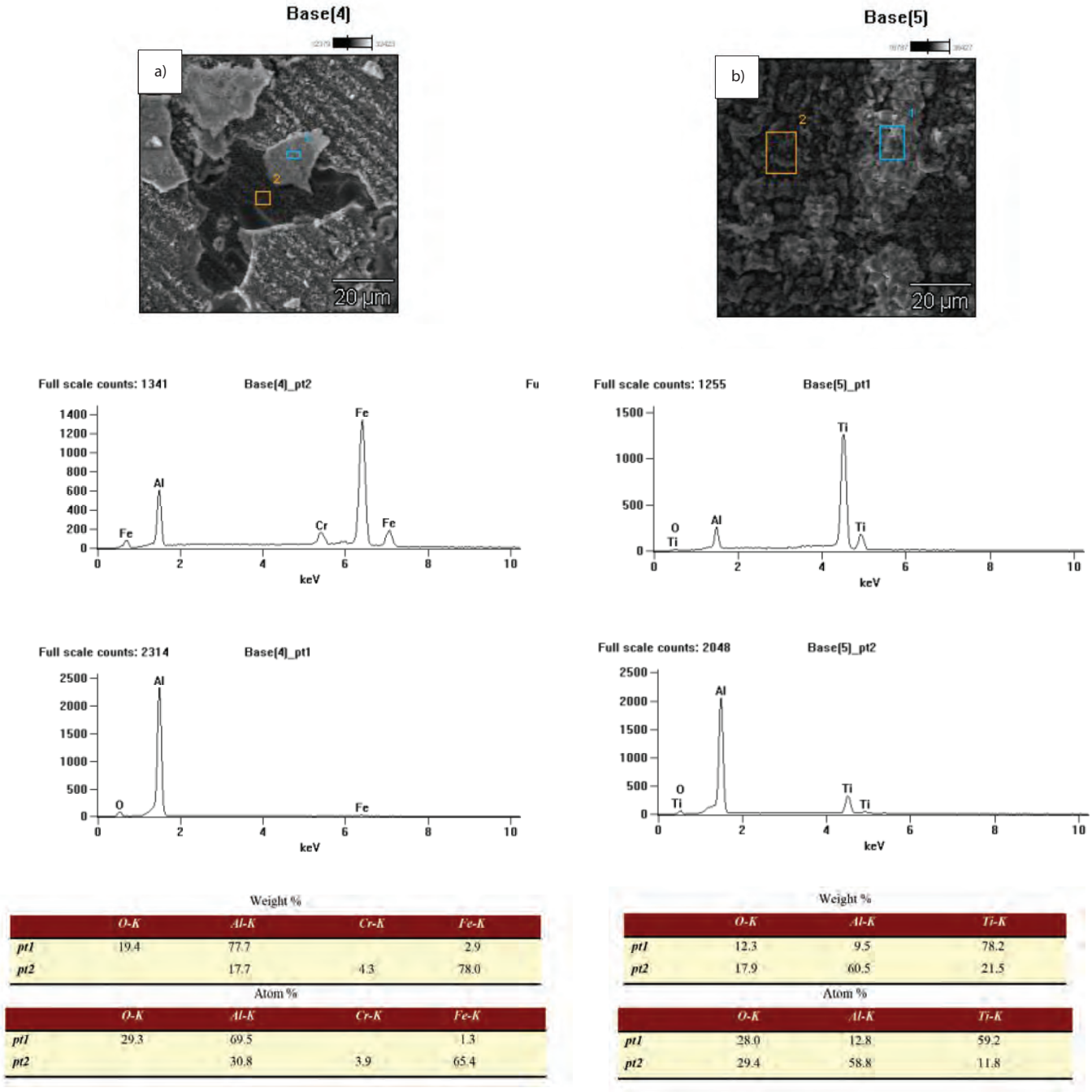

Weight %

	O-K	Al-K	Cr-K	Fe-K
pt1	19.4	77.7		2.9
pt2		17.7	4.3	78.0

Atom %

	O-K	Al-K	Cr-K	Fe-K
pt1	29.3	69.5		1.3
pt2		30.8	3.9	65.4

Weight %

	O-K	Al-K	Ti-K
pt1	12.3	9.5	78.2
pt2	17.9	60.5	21.5

Atom %

	O-K	Al-K	Ti-K
pt1	28.0	12.8	59.2
pt2	29.4	58.8	11.8

Fig. 4. Chemical composition X-ray microanalysis results of oxidation products from alloys oxidized at 1000°C: a) $Fe_{40}Al_5Cr_{0.2}ZrB$, b) TiAl

Rys. 4. Wyniki mikroanalizy rentgenowskiej składu chemicznego produktów utleniania w temperaturze 1000°C stopów: a) $Fe_{40}Al_5Cr_{0.2}ZrB$, b) TiAl

oxidation at 1000°C for 500 h (Fig. 1h). For the $Fe_{40}Al_5Cr_{0.2}ZrB$ alloy, the sample surface after 50 h of oxidation showed the most homogeneous scale structure (Fig. 1a). The greatest adhesion of the scale to the substrate was observed on the TiAl sample after annealing for 100 h – its surface was completely covered with an oxide layer. The reason for the crumbling and flaking of the scale on the $Fe_{40}Al_5Cr_{0.2}ZrB$ samples may have been higher compressive stresses caused by the cooling process of the test samples, or lower adhesion of the scale to the substrate [8].

Oxidation kinetics had a similar pattern, but $Fe_{40}Al_5Cr_{0.2}ZrB$ alloy was more resistant to oxidation than TiAl alloy (Fig. 2). It was shown that, depending on the annealing time, the oxidation product morphology of alloys on the FeAl and TiAl intermetallic phase (Fig. 3) differed, although aluminum was selectively oxidized in both cases (Fig. 4). The surface of $Fe_{40}Al_5Cr_{0.2}ZrB$ alloy after oxidation for 200 h and 500 h showed the most areas where the oxide layer was chipped or flaked (Fig. 3e, 3g). The heterogeneity of the oxide layer's surface structure may be due to the build-up of scale on the sample, causing its adhesion to decrease. On the TiAl alloy samples, the scale layer did not spall; however, it was a two-component alloy. Determining the morphology of the TiAl multi-component system alloy after high-temperature oxidation requires further research. Compressive stresses are responsible for the formation of needles (so-called whiskers) in the $Fe_{40}Al_5Cr_{0.2}ZrB$ alloy [9, 10]. In assessing the surface condition of $Fe_{40}Al_5Cr_{0.2}ZrB$ alloy, it should be noted that crystallites of various sizes became visible; particularly small crystallites were observed on the sample after 100 h of annealing. All tested samples of both alloys were characterized by multilayer

scaling: subsequent layers were visible where the first layer had eroded, especially where the oxide layers had flaked off. The surface morphology of $Fe_{40}Al_5Cr_{0.2}ZrB$ and TiAl alloys differed significantly; in the titanium-aluminum alloy, no needles characteristic of Al_2O_3 oxide were observed, but crystallite-like structures.

5. Conclusion

Based on the research and analysis of the results, the following conclusions have been formulated:

1. $Fe_{40}Al_5Cr_{0.2}ZrB$ intermetallic phase matrix alloy forms a passive aluminum oxide layer after oxidation in air at 1000°C, while a more complex scale is formed on TiAl intermetallic phase alloy. However, it requires a more detailed analysis, mainly using transmission electron microscopy, which includes determining the chemical and phase composition of corrosion products.
2. Oxidation of both $Fe_{40}Al_5Cr_{0.2}ZrB$ intermetallic phase-based alloy and TiAl alloy at 1000°C, regardless of the process time, results in selective aluminum oxidation. To the extent identifiable by the test methodology used, the presence of other elements that may be part of the scale was not demonstrated.
3. Annealing of $Fe_{40}Al_5Cr_{0.2}ZrB$ alloy for 100 h at 1000°C resulted in the formation of a passive layer that adhered more strongly to the substrate than after oxidation for 200 h. After 500 h, the passive layer came off, most likely due to thermal stresses associated with different coefficients of thermal expansion.
4. The morphology of oxidation products for $Fe_{40}Al_5Cr_{0.2}ZrB$ alloy and TiAl alloy oxidized at 1000°C varies. Determining the type of aluminum oxide depending on the type of parent material requires further research.

Part of the results of the research described in the article were obtained in the course of research conducted by Kamil Mamerski in the framework of his master's thesis entitled *High-Temperature Corrosion Resistance of Fe-Al, Ti-Al Intermetallic Phase Matrix Alloys* (2022), carried out under the direction of the author of this publication.

BIBLIOGRAPHY

[1] A. Gil. 2009. *Wysokotemperaturowa korozja stopów TiAl*. Kraków: Wydawnictwo Naukowe Akapit.
[2] R. Viswanathan, R. Purget, U. Rao. 2002. *Materials for Ultra-Supercritical Coal-Fired Power Plants*. In: J. Lecomte-Beckers, M. Carton, F. Schubert, P.J. Ennis (eds.). *Materials for Advanced Power Engineering 2002: Proceedings of the 7th Liège Conference*. Jülich, Germany: Forschungszentrum Jülich.
[3] S. Jóźwiak. *Aluminki żelaza. Sekwencja przemian fazowych w procesie nieizotermicznego spiekania proszków żelaza i aluminium*. Warszawa: Bel Studio.
[4] J. Cebulski, D. Pasek, M. Bik, K. Świerczek, P. Jeleń, K. Mroczka, J. Dąbrowa, M. Zajusz, J. Wyrwa, M. Sitarz. 2020. "*In-Situ* XRD Investigations of FeAl Intermetallic Phase-Based Alloy Oxidation". *Corrosion Science* 164: 108344. DOI: 10.1016/j.corsci.2019.108344.
[5] E. Godlewska, R. Mania, S. Szczepanik. 1999. "Selected Properties of Fe-Al Intermetallics Prepared by Various Processing Routes". *Proceedings of International Conference on Environmental Degradation of Engineering Materials*. Gdańsk–Jurata.
[6] M. Rozmus. 2006. *Mechaniczne wytwarzanie stopów na osnowie faz międzymetalicznych z układu Ti-Al-Nb i ich charakterystyka*. Rozprawa doktorska. Kraków: Akademia Górniczo-Hutnicza, Wydział Inżynierii Metali i Informatyki Przemysłowej.
[7] K. Mamerski. 2022. *High-Temperature Corrosion Resistance of Fe-Al, Ti-Al Intermetallic Phase Matrix Alloys*. Master's thesis. Katowice: Silesian University of Technology, Faculty of Materials Engineering.
[8] D. Pasek. 2021. *Utlenianie stopu na osnowie fazy międzymetalicznej FeAl w powietrzu i parze wodnej*. Rozprawa doktorska. Katowice: Politechnika Śląska.
[9] M. Homa. 2008. „Żaroodporność i żarowytrzymałość stali typu Fe-Cr-Al w warunkach utleniających; aktualny stan i perspektywy badań". *Prace Instytutu Odlewnictwa* 48(3): 57–85.
[10] B. Surowska. 2002. *Wybrane zagadnienia z korozji i ochrony przed korozją*. Lublin: Politechnika Lubelska. http://www.bc.pollub.pl/Content/254/korozja.pdf (dostęp: listopad 2022).